

Past climate changes, population dynamics and the origin of Bison in Europe

Diyendo Massilani^{1,*}, Silvia Guimaraes^{1,*}, Jean-Philip Brugal², E. Andrew Bennett¹, Malgorzata Tokarska³, Rose-Marie Arbogast⁴⁺, Gennady Baryshnikov⁵⁺, Gennady Boeskorov⁶⁺, Jean-Christophe Castel⁷⁺, Sergey Davydov⁸⁺, Stéphane Madelaine⁹⁺, Olivier Putelat¹⁰⁺, Natalia N. Spasskaya¹¹⁺, Hans-Peter Uerpmann¹²⁺, Thierry Grange^{1,§}, Eva-Maria Geigl^{1,§}

¹Institut Jacques Monod, UMR7592, CNRS, University Paris Diderot, Epigenome and Paleogenome group, 15 rue Hélène Brion, 75013 Paris, France

²CNRS, USR 3336 IFRA (Institut Français de Recherche en Afrique ; Nairobi, Kenya) & Aix-Marseille Université, UMR 7269 LAMPEA (Labo.Méd.de Préhistoire, Europe-Afrique ; Aix-en-Provence, France) Maison Méditerranéenne des Sciences de l'Homme, BP 674, 13094, Aix-en-Provence cedex 2, France

³Mammal Research Institute Polish Academy of Sciences, Genetics and Evolution Department, Waszkiewicza 1, 17-230 Białowieża, Poland

⁴CNRS/UMR 7044/MISHA, 5 allée du Général Rouvillois, 67083 STRASBOURG Cedex

⁵Zoological Institute, Russian Academy of Sciences, 199034 Saint Petersburg, Russia

⁶Diamond and Precious Metal Geology Institute of the Siberian Branch of the RAS, Yakutsk, Russia

⁷Muséum d'histoire naturelle de Genève (MHN), Département d'Archéozoologie, route de Malagnou 1, 1208 Genève, Switzerland

⁸North-East Science Station, Pacific Institute of Geography, Far East Branch, Russ. Ac. Sci., 678830 Cherskiy, Russia

⁹Musée national de Préhistoire, 24620 Les Eyzies de Tayac-Sireuil, France

¹⁰Pôle d'Archéologie Interdépartemental Rhénan, 67600 Sélestat, France and UMR 7041 ArScan - Archéologies environnementales - Maison de l'Archéologie et de l'Ethnologie, 92023 Nanterre, France

¹¹Zoological Museum of Moscow Lomonosow, State University, Bolshaya Nikitskaya Str., 6, Moscow 125009 Russia

¹²Institut für Ur- und Frühgeschichte und Archäologie des Mittelalters, Abteilung Ältere Urgeschichte und Quartärökologie, Zentrum für Naturwissenschaftliche Archäologie, Rümelinstr. 23, 72070 Tübingen, Germany

+alphabetical order

Corresponding authors: Thierry Grange and Eva-Maria Geigl,
Institut Jacques Monod, Epigenome and Paleogenome group, 15 rue Hélène Brion, 75013 Paris, France; Fax: +33-157278101
email: thierry.grange@ijm.fr; eva-maria.geigl@ijm.fr

*equal contribution

§equal contribution

Keywords: ancient DNA, bison, population dynamics, evolution, next generation sequencing, sequence capture,

Running title: European bison history since the late Pleistocene

1 Abstract

2 Climatic and environmental fluctuations as well as anthropogenic pressure have led to the extinction
3 of much of Europe's megafauna. Here we show that the emblematic European bison has experienced
4 several waves of population expansion, contraction and extinction during the last 50,000 years in
5 Europe, culminating in a major reduction of genetic diversity during the Holocene. Fifty-seven
6 complete and partial ancient mitogenomes from throughout Europe, the Caucasus and Siberia reveal
7 that three populations of wisent (*Bison bonasus*) and steppe bison (*B. priscus*) alternated in Western
8 Europe correlating with climate-induced environmental changes. The Late Pleistocene European
9 steppe bison originated from northern Eurasia whereas the modern wisent population emerged from
10 a refuge in the southern Caucasus after the last glacial maximum. A population overlap in a transition
11 period is reflected in ca. 36,000 year-old paintings in the French Chauvet cave. Bayesian analyses of
12 these complete ancient mitogenomes yielded new dates of the various branching events during the
13 evolution of *Bison* and its radiation with *Bos* that lead us to propose that the genetic affiliation between
14 the wisent and cattle mitogenomes result from incomplete lineage sorting rather than post-speciation
15 gene flow.

16 Significance

17 Climatic fluctuations during the Pleistocene had a major impact on the environment and led to multiple
18 megafaunal extinctions. Through ancient DNA analyses we decipher these processes for one of the
19 largest megafauna of Eurasia, the bison. We show that Western Europe was successively populated
20 during the Late Pleistocene by three different bison clades or species originating from the Caucasus
21 and North-Eastern Europe that can be correlated to major climatic fluctuations and environmental
22 changes. Aurignacian cave artists were witnesses to the first replacement of bison species ~35,000
23 years ago. All of these populations went extinct except for one that survived into the Holocene where
24 it experienced severe reductions of its genetic diversity due to anthropogenic pressure.

26 Introduction

27 Drastic climatic fluctuations during the Pleistocene in the northern hemisphere led to population
28 contractions, extinctions, reexpansions and colonizations of fauna and flora (1). Bison, along with other
29 large ungulates thrived during the Middle and Late Pleistocene (2). Numerous cave paintings and
30 engravings in France and Spain, such as those in the caves of Chauvet, Lascaux and Altamira, attest to
31 the important role this impressive animal played for the late Paleolithic hunter-gatherers. The steppe
32 bison (*Bison priscus* (Bojanus, 1827)) appears in the fossil record during the Early Middle Pleistocene,
33 replacing another archaic but smaller forest-adapted bison (*B. schoetensacki*(3)), which went extinct
34 ca. 700 kiloyears ago (kya) (4). Since *B. priscus* was adapted to the cold tundra-steppe, occurrence of
35 its remains is considered indicative of open environments (5). It roamed over Europe and Asia, and
36 also crossed the Bering Strait during the Middle Pleistocene to populate North America where it
37 evolved into the American Bison *B. bison* (3, 6, 7). The numerous fossil remains display a pronounced
38 sexual dimorphism, and a large initial body size, gradually decreasing throughout the Pleistocene (5).
39 Differences in morphology related to climatic, environmental and topographic conditions have led
40 several authors to propose a high diversity for the Pleistocene cold-steppe bison expressed as
41 subspecies or ecomorphotypes (5, 6).

42 The taxonomy, evolutionary history and paleobiogeography of the genus *Bison* in Eurasia, and of
43 the European bison or wisent *B. bonasus* (Linnaeus, 1758) in particular, is still patchy, despite a rich
44 fossil record and its current endangered status (e.g., (8-11)). Indeed, two opposing hypotheses on the
45 evolution of bison in Eurasia coexist (2). Traditionally, it has been considered that bison developed
46 within one single phylogenetic line (*B. schoetensacki* – *B. priscus* – *B. bonasus*), but it has also been
47 proposed that at least two parallel lines of bison existed, one being the line of forest bison from
48 *B. schoetensacki* (Freudenberg, 1910) to the recent *B. bonasus* and the other being the line of the
49 steppe bison *B. priscus* (for a review see (2)). Thus, the phyletic relationships between *B. schoetensacki*,
50 *B. priscus* and *B. bonasus*, as well as the approximate date and geographical origin of the wisent remain

51 elusive, due in part to the limited power of paleontological studies to resolve species-level mammalian
52 taxonomy issues or detect broad-scale genetic transitions at the population level (12).

53 *B. priscus* disappeared from the fossil record of Western Europe at the end of the Pleistocene,
54 around 12 – 10 kya, and relict populations of *B. priscus* seem to have survived until the beginning of
55 the Middle Holocene (7-6 kya) in Siberia (i.e., (13, 14)). In Europe, *B. priscus* is believed to have been
56 replaced at the end of the Pleistocene or during the Holocene by the morphologically (eidonomically)
57 distinguishable wisent, *B. bonasus* (2, 10, 15, 16). At least two sub-species are recognized: (i)
58 *B. b. bonasus* Linnaeus, 1758 from the Lithuanian lowland and the Polish Białowieża ecosystem, and
59 (ii) the Caucasian highland *B. b. caucasicus* (Turkin and Satunin, 1904). (17). *B. priscus* was adapted to
60 forest-steppe and steppe, and *B. bonasus* to forest and mountain-forest environments. *B. priscus* and
61 *B. bonasus* are anatomically much closer to each other than to other more ancient bison, such as
62 *B. schoetensacki*. *B. bonasus* has a relatively more massive rear quarter and shorter horns compared
63 to *B. priscus* which has longer and slightly curved horns and a smooth double-humped appearance (15,
64 16). *B. priscus* and *B. bison* (Linnaeus, 1758), which are grazers, have a lower head position than
65 *B. bonasus*, which is a mixed feeder (18). It is, however, very difficult to assign fossil bison bones to
66 either species (2). Cave paintings of bison from caves in France and Spain are often classified as
67 belonging to either *B. priscus* or to *B. bonasus* (19). The diversity of the cave art depictions and the
68 large range of their occurrence is interpreted as indicating an origin of *B. bonasus* in the area between
69 southern Europe and the Middle East and of its existence well before the end of the Late Pleistocene
70 at a time when *B. priscus* was still present (19).

71 Both extant bison species narrowly escaped extinction. The American *B. bison* was almost wiped
72 out during the 19th century through commercial hunting and slaughter, but also introduced bovine
73 diseases and competition with domestic livestock (20). The wisent as well almost went extinct at the
74 beginning of 20th century. Indeed, similar to other large herbivores, such as the aurochs, intensification
75 of agriculture since the Neolithic pushed the wisent into the forests of Eastern Europe (18) where it

76 was strictly protected for a few centuries as a royal game animal (11). During the First World War,
77 however, diminished population size followed by poaching led to its extinction in the wild (11). Of the
78 54 remaining wisents living in captivity at the beginning of the 1920s, the descendants of just 12
79 animals constitute the entire extant population (11).

80 The wisent is still poorly characterized genetically. While genetic markers from the autosomes and
81 Y chromosomes of American bison and wisent are closer to each other than to the other members of
82 the genus *Bos* and they can reproduce and give rise to fertile offspring, their mitochondrial genomes
83 are phylogenetically separated (9, 21, 22). Indeed, mitochondrial sequences of the American bison and
84 the yak *Poephagus mutus* f. *grunniens* (Linnaeus, 1758) form a distinct cluster while the wisent
85 occupies a phylogenetic position closer to *Bos primigenius* f. *Taurus* (Linnaeus, 1758), a phenomenon
86 that has been explained by incomplete lineage sorting or ancient hybridization (21, 22). European,
87 Siberian and American *B. priscus* mitogenomes were shown to be phylogenetically closer to *B. bison*
88 than to *B. bonasus* (7, 14, 23).

89 Ancient DNA (aDNA) studies have the potential to better resolve taxonomy than paleontological
90 studies, in particular at the species level, and have revealed a far more dynamic picture of megafaunal
91 communities, biogeography and ecology, including repeated localized extinctions, migrations, and
92 replacements (e.g., (12) and citations therein). To better understand the phylogeography and
93 evolution of the wisent and to reconstruct its origin, we performed a study of the mitochondrial
94 genome over the past 50,000 years (50 kyrs) across Europe and Asia. Using Pleistocene skeletal
95 remains from Siberia (Yakutia), the Caucasus and Western Europe (France, Switzerland) as well as
96 Neolithic and Medieval samples from France, and also pre-bottleneck *B. bonasus* samples from the
97 early 20th century from the Polish lowland and the Caucasian highland lines, we constructed a
98 phylogenetic framework based on both the hypervariable region of the mitochondrial DNA as well as
99 complete mitochondrial genomes of selected specimens. Our results give new insights into the climate-
100 driven dynamics of the bison in Europe.

101 Results

102 The evolution of the mitochondrial hypervariable region

103 We analyzed 57 paleontological and 25 historical specimens (see SI Table 1) targeting the
104 mitochondrial hypervariable regions with four fragments of at most 150 bp. We obtained a 367 bp-
105 long sequence from 43 specimens, and smaller sequences from 13 additional ones (SI Fig. 1). A
106 Maximum Likelihood phylogenetic tree was constructed using these sequences (Fig. 1). Three clades
107 can be clearly distinguished. The first clade *Bp*, which is more divergent from the other two, comprises
108 samples from Pleistocene Yakutia (Siberia) and from southern France (Berbie and lower stratigraphic
109 layers of Gral), dating from 44 to 26 kya and from 39 to 15 kya, respectively. Clade *Bp* corresponds to
110 the *B. priscus* lineage previously described for Siberia, North America and Europe (7, 23). The French
111 and Siberian sequences of this clade are phylogenetically close and lack a phylogeographic structure.
112 This reveals that a relatively homogeneous population of steppe bison was distributed during the Late
113 Pleistocene not only in Siberia and northern America but also throughout the entire northern part of
114 the Eurasian continent up to its most-western part, France.

115 The two other clades, *Bb1* and *Bb2*, are more closely related to the extant wisent *B. bonasus*. The
116 *Bb1* clade, significantly divergent from *Bb2*, contains most of the specimens from the Mezmaiskaya
117 cave Northwest of the Caucasus in Russia, dating from ca. 48 to 43 kya, as well as seven specimens
118 from southern France (Arquet, Plumettes), dating from ca. 47 to 34 kya. Thus, the geographical range
119 of the *Bb1* clade stretched from the northern Caucasus to the south of France at its latest, from 48 to
120 34 kya during the overall mild Marine Isotope Stage (MIS) 3 (ranging from 57 to 29 kya (24),
121 http://www.lorraine-lisiecki.com/LR04_MISboundaries.txt). None of the haplotypes of the *Bb1* clade
122 was found in the more recent specimens, suggesting that the corresponding population may have been
123 the first to disappear. This *Bb1* population in France was apparently replaced by the steppe bison of
124 the *Bp* clade around 30 kya, the latter remaining there throughout the glacial period of MIS2 (ranging
125 from 29 to 14 kya (24), http://www.lorraine-lisiecki.com/LR04_MISboundaries.txt).

126 Clade *Bb2* includes both ancient specimens from the Caucasus and Western Europe as well as all
127 recent and extant *B. bonasus* specimens. Nearly all ancient samples belonging to this clade are distinct
128 from the more recent populations and include a ca. 49 ky-old specimen from the Mezmaiskaya cave,
129 two specimens from the Kudaro cave in the central part of the southern slope of the Greater Caucasus
130 dated at 38 and 22 kya, and specimens from Western Europe: one specimen from the Kesslerloch cave
131 (Switzerland) dated at 14 kya, and, in France, two bison from the upper stratigraphic sequence of the
132 Gral dated at 12 kya, two 5.2kyr-old bison samples from the Neolithic site of Chalain, as well as three
133 medieval (7th-8th century CE) specimens from Alsace. The members of this clade represent the western
134 European Pleistocene-Holocene lineage of *B. bonasus* and display a high mitochondrial diversity. This
135 lineage appears to have replaced the *B. priscus* lineage, at least in France, at the end of the Upper
136 Pleistocene between 15 and 12 kya, coinciding with the onset of a more temperate climate, and to
137 have persisted in France up to the Middle Ages. Apart from the sequence found in the sample from
138 Kesslerloch (12.2 kya), none of the ancient *Bb2* sequences are present in the extant mitochondrial gene
139 pool.

140 Within the *Bb2* clade, a compact group of closely related sequences, comprise the Upper
141 Pleistocene Kesslerloch specimen and the 1898-1917 pre-bottleneck wisents from both Poland and
142 the Caucasus that almost became extinct at the end of the First World War. Five out of 24 of these pre-
143 bottleneck bison have a hypervariable region (HVR) sequence identical to that of extant *B. bonasus*,
144 whereas the rest differ from the extant sequence by only one or two single nucleotide polymorphisms
145 (SNPs). Thus, the pre-bottleneck mitochondrial diversity appears only slightly higher than at present
146 and much lower than that observed in older samples. The 14 kyr-old Kesslerloch specimen reveals the
147 first occurrence of the mitogenome lineage of the extant *B. bonasus* population. Thus, the modern
148 population corresponds to a minor fraction of the diversity that was present in Europe during the Late
149 Pleistocene when *B. bonasus* replaced *B. priscus*.

150 A major reduction in the intrapopulation diversity is apparent from the Late Pleistocene to the early
151 20th century (Table 1). The Pleistocene populations of Siberia, the Caucasus and Europe are

152 characterized by a high diversity at both the haplotype ($H=1.00$) and nucleotide levels (as estimated
153 with Π and various Theta estimators), the nucleotide diversity of the European *B. priscus* being lower
154 than that of its Siberian population. The Western European Holocene population of *B. bonasus*
155 experienced a major reduction of its diversity between the Middle Ages and the beginning of the 20th
156 century.

157 We performed a phylogenetic analysis of the HVR under the Bayesian framework estimating
158 mutation and population history parameters from temporally spaced sequence data using all dated
159 ancient and modern bison HVR sequences present in GenBank in 2015 in combination with the data
160 from the current study (Fig. 2). The resulting tree shows a bifurcation between the *Bison bonasus* and
161 *Bison priscus/bison* mitogenome lineages about 1.0 Mya [95% highest posterior density interval (HPD):
162 1.5-0.7] (Table 2 and Fig 2). The most recent common ancestor (MRCA) of the Eurasiatic and the
163 American *B. priscus* clades is estimated here at 151 kya [193-119], which is in agreement with a
164 previous estimate of 136 ky [164-111] that was also based on the HVR (7). *B. priscus* from America and
165 Siberia group in distinct clades, and the modern American bison descended from a small subgroup of
166 a once diverse American population, as previously proposed (7). The Late Pleistocene European
167 *B. priscus* corresponds to a subset of the Siberian population.

168 The phylogenetic analyses of the *B. bonasus* haplotypes reveal that the ancient Caucasian
169 population had a deep root and was highly diverse. Based on the HVR, the age of the MRCA of the *Bb1*
170 and *Bb2* clades is estimated at 438 [643-284] kya, which is significantly older than the MRCA of
171 *B. priscus* (Fig. 2 and Table 2). This observation indicates that the Upper Pleistocene Caucasian
172 population had a deeper root than the contemporaneous and more northern *B. priscus* population,
173 even though the latter one may have occupied in the past a much larger territory from Western Europe
174 to the American continent. The *Bb2* clade encompasses several branching events, the separation of a
175 branch represented by a ca. 50 kyr-old northern Caucasus specimen from Mezmaiskaya occurring first,
176 i.e., 105 [158-75] kya, followed, 61 [89-43] kya, by the separation of a branch represented by a ca. 37.8

177 kyr-old specimen from the Kudaro cave in the southern Caucasus. Then, 42 [60-26] kya, the subgroup
178 comprising an 22.2 ky-old specimen from the Kudaro cave as well as all French specimens between
179 12.4 to ca. 1.2 kya separated from the haplogroup encompassing the modern *B. bonasus* sequences.
180 Finally, in this later haplogroup, the 14 ky-old Kesslerloch specimen and the early 20th century Central
181 European and Caucasus specimens have a MRCA estimated at 16 [33-14] kya. This sequential order of
182 the radiation events and the previously mentioned reduction of the population diversity indicates that
183 at the transition between the Pleistocene and the Holocene, Western and Central Europe were
184 populated by a subset of a wisent population established in an area of southern Asia including the
185 Caucasus, and that only a part of this population survived into the 20th century.

186 The evolution of the Bison clades based on entire mitogenomes

187 To render this phylogeny and dating scenario more robust, we used biotinylated RNA probes
188 synthesized from the complete mitogenome of *B. p. taurus*, and optimized a sequence capture
189 approach to recover complete mitogenome sequences from seven well-preserved 50 to 12 kyr-old
190 specimens representative of the various clades and radiation events defined above. We performed a
191 Bayesian phylogenetic analysis of these mitogenomes and of two recently published *B. priscus*
192 mitogenomes (14, 23) together with those of modern *B. bison* and *B. bonasus*, *B. p. taurus*, and
193 *P. grunniens* complete mitogenomes present in GenBank in 2015 (Fig. 3). As previously observed with
194 modern sequences (9, 21, 22), the *B. bonasus* mitogenome lineage is more closely related to the
195 *Bos p. taurus* lineage than to the *B. priscus* – *B. bison* lineages. The Bayesian analysis reveals, however,
196 that there is a significant overlap (35 to 40%) of the 95% HPD intervals of the dates estimated for the
197 node separating the *Bos p. taurus*–*B. bonasus* and the *B. priscus* – *B. bison* lineages, estimated here at
198 944 [1090-810] kya, and the node separating the *B. p. taurus* and *B. bonasus* lineages, estimated here
199 at 786 [908-668] kya. Such an overlap suggests that the two bifurcation events may have occurred
200 within a relatively short evolutionary period, thus increasing the likelihood that these two events
201 preceded the major separation of the *B. p. taurus* and *Bison* species. This peculiar affiliation pattern of
202 mitogenomes renders the incomplete lineage sorting hypothesis a parsimonious interpretation (see

203 SI Fig. 2). The *Bison priscus/bison* and yak (*P. grunniens*) mitogenome lineages separated from a
204 common ancestor dated at ca. 328 kya [378-272]. For the *Bison* mitogenomes, the dates of the nodes
205 estimated with complete mitogenomes are often younger than those estimated using only the HVR
206 (Table 2). For instance, the common ancestor of the *Bb1* and *Bb2* clades is estimated at 250 kya [287-
207 211] when comparing full mitochondrial genomes, rather than 438 kya [643-284] calculated from only
208 HVR sequences. Similarly, the common ancestor of the Eurasian *B. priscus* and the modern American
209 bison is estimated at 115 [135-95] kya rather than 151 [193-119] kya. In contrast, the various branching
210 events within the *Bb2* clade show non-significant differences (given the overlap of the HPD) between
211 the two series of date estimations: 87 [97-75] kya instead of 105 [158-75] kya for the ancestor of the
212 North and South Caucasian specimens, 63 [70-52] kya instead of 61 [89-43] kya for the ancestor of the
213 South Caucasus and Holocene European specimens, and 37 [42-29] kya instead of 42 [60-26] kya for
214 the ancestor of the Holocene European specimens. The discrepancies between the date estimates for
215 several nodes depending on the genetic region used may be partly due to the differences in the
216 number of individual sequences studied in the two series. The major source of discrepancy, however,
217 appears to be due to an irregular rate of evolution of the HVR. Indeed, even though the clock rates
218 estimated for the HVR are similar when either the HVR alone or as a partition of the complete
219 mitogenome is used (respectively 5.4 [3.9-6.9] and 4.6 [3.7-5.6] E-7 per site x year), the individual HVRs
220 show distinct evolutionary rates. When the distribution throughout the mitogenome of the SNPs
221 distinguishing individual bison mitogenomes from the *B. p. taurus* mitogenome as an outgroup are
222 compared, the number of SNPs accumulated in the HVR can vary up to two-fold between individual
223 sequences whereas the rest of the mitogenome is equally distant to the outgroup (SI Fig. 3). For
224 example, there are twice as many mutations accumulated in the HVR subregion (15900-16100) of the
225 Mez 128, Gral 232 and Yaku 118 mitogenomes than in the ones of the Mez130 and Gral 125 specimens.
226 Whatever the underlying mechanism responsible for these differences of the evolutionary rate of this
227 particular region of the mitogenome, this phenomenon limits the reliability of the dating estimations
228 based solely on the HVR.

229 Complete mitogenomes confirm the observation made with the HVR sequences that the European
230 *B. priscus* specimens from the Late Pleistocene were more homogeneous genetically than the
231 contemporaneous Siberian population. Indeed, the two French mitogenomes from the Gral (Gral232)
232 and Trois-Frères cave (23) are very similar, with only 19 SNPs distinguishing them, whereas the two
233 Siberian mitogenomes (Yaku118 and Rauchua (14)) are much more divergent with eight-fold more
234 SNPs distinguishing them (153 SNPs). Strikingly, the age of the MRCA of the 26.7 kyr-old Yakutian
235 sample and the 20 to 15 kyr-old French *B. priscus* samples is estimated at 58 [66-47] kya. Since the
236 MRCA of these sequences is also the MRCA of the group of HVR sequences comprising two additional
237 Yakutian and all other French *B. priscus* samples (see Fig. 1), this indicates that the steppe bison
238 inhabiting France between 39 and 15 kya originated from a migration from North-East Eurasia that
239 occurred not earlier than 58 [66-47] kya. Presumably, the low genetic diversity of the Western
240 European *B. priscus* population is due to a founder effect during this migration.

241 The phylogenetic relationships between the *B. bonasus* mitogenomes indicate that modern wisent
242 in central Europe are more closely related to the Late Pleistocene/Holocene Western European
243 population than to the Late Pleistocene Caucasian population. Indeed, the 14 kyr-old specimen from
244 the site of Kesslerloch at the Swiss-German border is closely related to modern wisent, with only 15
245 SNPs distinguishing the ancient and modern mitogenome sequences. This demonstrates that the range
246 of the ancestral population of the modern wisent encompassed Middle Europe 14 kya. The Late
247 Pleistocene Caucasian population was highly diverse with a deep root separating most of the
248 specimens from the Mezmaiskaya cave in the northern Caucasus, belonging to the *Bb1* clade, from the
249 specimens from the Kudaro cave in the southern Caucasus, belonging to the *Bb2* clade, and including
250 a specimen from the northern Caucasus: 342 SNPs distinguished the Mez128 (*Bb1*) and the Mez130
251 (*Bb2*) mitogenomes and 105 SNPs distinguished the northern (Mez 130) and southern Caucasian
252 (Kud136) mitogenomes of the *Bb2* clade. In contrast, the members of the *Bb2* clade in Western Europe
253 were more similar, with only 39 SNPs distinguishing the French (Gral125) and Swiss (KSL) specimens,
254 in agreement with the reduction of diversity that we observed when comparing the HVR of the

255 Western European and Caucasian *B. bonasus* populations. Thus, complete mitogenomes confirm the
256 observations from the HVR analyses of a larger sample size while providing a more accurate
257 phylogenetic analysis, in particular with respect to the dating of the MRCA of the various mitogenomes.

258 Discussion

259 European bison populations turnover during the late Pleistocene and the 260 Holocene

261 Our results enable us to propose a scenario for the evolutionary history of the bison in Europe that
262 is related to the climatic fluctuations and the resulting environmental changes of the Late Pleistocene
263 and the Pleistocene/Holocene transition as summarized in Figure 4. We observe striking regional and
264 temporal differences in the major clades and distinguish three periods, particularly in France. The first
265 period, from at least 47 kya to about 34 kya, was characterized by the dominance of a divergent
266 *B. bonasus* lineage belonging to the *Bb1* clade in both southern France (Arquet and Plumettes, 7 *Bb1*
267 out of 7 samples) and the northern Caucasus (Mezmaiskaya, 5 *Bb1* and 1 *Bb2* out of 6 samples). This
268 lineage was absent from the samples from later periods indicating that the corresponding population
269 was the first to disappear. For the same time period, the steppe bison mitotype *Bp* was the sole
270 mitotype found in Siberia and northern Eurasia (27/27 samples dated from 66 to 34 kya (7)). This
271 period, encompassing most of MIS3, is characterized by oscillating shorter glacial and longer
272 interstadial periods, the latter lasting more than one thousand years (glacial interstadial GI15 to GI8
273 (12, 25) and Fig. 4). During the warmer periods, southern France and the northern Mediterranean coast
274 were covered by deciduous coniferous non-continuous forests, and central France and central Europe
275 by coniferous open woodland (26). The steppe bison *B. priscus* was dominant in France during the
276 following period that lasted until the end of the Last Glacial Maximum (LGM) at 14.7 kya (7 out of 7
277 samples, plus 1 out of 1 in (23)). These bison were closely related to the Siberian sample from Yakutia
278 from the same period, the whole mitogenome of which we analyzed (99.4% identity between the
279 Yaku128 and Gral232 mitogenomes). HVR comparisons between the French and Siberian and North
280 American samples (7) reveal that the French *B. priscus* mitotypes are closely related to those of the
281 Siberian samples (Fig. 2), indicating that the Western European territory was colonized by a
282 subpopulation of the steppe bison from the northern Eurasian continent. The age estimated from full
283 mitogenomes for the MRCA of the French and Siberian samples is 56 [64-46] kya, indicating that this

284 colonization involved a population that separated from the Siberian population more recently than
285 ca. 56 kya and suggesting a lower limit for the arrival in France of these steppe bison. In contrast,
286 specimens older than 60 kya assigned to *B. priscus* in the fossil record of Western Europe presumably
287 must have belonged to a distinct population that was not the direct ancestor of this *B. priscus*
288 population that occupied Western Europe during the cold spells of MIS2. At the end of MIS3, around
289 32 kya, the climate became colder on average and the warmer interstadials were shorter, lasting only
290 a few hundred years. Then, between 27 and 14.7 kya, a second, long glacial period followed that
291 comprised two phases. In the first phase, the tree cover was patchy and incomplete, with a high
292 proportion of steppe vegetation, whereas the second, a full glacial phase, was characterized by sparse
293 grassland and open steppe tundra in southern and northern Europe, respectively (27). While during
294 this period the steppe bison *B. priscus* occupied the territory previously occupied by *B. bonasus* in
295 Western Europe, *B. bonasus* remained nevertheless present in the southern Caucasus, even during the
296 LGM. Indeed, in our samples, two out of two specimens from the southern Caucasus belonged to the
297 *Bb2* clade, which we found to be present at low frequency at an earlier period in the northern
298 Caucasus. Finally, during the third period, starting at the end of the MIS2 and lasting up to the present,
299 *B. bonasus* of the *Bb2* clade expanded again into Western Europe, as we detected it in the 14 kyr-old
300 specimen from Switzerland at the beginning of the Bølling-Allerød interstadial period (14.7 to 12.7
301 kya). The more recent specimens from France belonged without exception to the *Bb2* clade (7 out of
302 7, dated between 12 kya to the Middle Ages). Strikingly, the sedimentary sequence of the French site
303 Gral recorded a population replacement: all specimens older than ca. 15 kya, before the Bølling-Allerød
304 interstadial, belong to the *B. priscus Bp* mitotype (5 out of 5), whereas all more recent ones, coinciding
305 with the onset of a more temperate climate at the end of the last glacial event (end of MIS2), belong
306 to the *B. bonasus Bb2* mitotype (2 out of 2, $P_{val} < 0.05$ with Fisher's test). The ancient French *Bb2*
307 population is significantly different from the one comprising the modern wisent and the ancient
308 Kesslerloch specimen (Fig. 1-3). Moreover, this subclade was not detected later than the Middle Ages,
309 suggesting that it went extinct in Western Europe with the disappearing local wisent. In contrast, the

310 distinct *Bb2* mitotype of the 14 kyr-old sample from Kesslerloch continued to exist up to present time.
311 It is the only remaining mitotype detected in both present-day wisent as well as in the specimens from
312 Poland and the Caucasus from the beginning of the 20th century prior to the last major bottleneck of
313 WWI.

314 The marked climatic variations that occurred during the Pleistocene implied drastic environmental
315 changes that triggered the profound reorganization of floral and faunal biomes at different geographic
316 and temporal scales. Response of biota to climatic stimuli was regionally/continentally distinct,
317 sometimes occurring synchronously but most often diachronously (e.g., (2, 28)). The repeated cyclical
318 climate changes progressively promoted landscape renewal, locally modifying, obliterating and
319 creating specific and varied ecological niches (28). The various expansions and contractions of bison
320 populations in response to these climatic fluctuations led to apparent alternating occupations of
321 Western Europe by either *B. priscus* or *B. bonasus* during the last 50 kyrs, each presumably originating
322 respectively from either a northeastern territory including Siberia, or a southern territory including the
323 Caucasus. We hypothesize that these alternating occurrences result from climate-driven changes of
324 two different habitats to which *B. priscus*, a grazer, and *B. bonasus*, a mixed feeder, were adapted, i.e.,
325 the open tundra-steppe for the first and open woodlands for the second. Indeed, the diet of *B. priscus*
326 during the LGM included typical steppe and grassland (C₃) vegetation and lichens (29), whereas the
327 wisent's diet in the Holocene was more flexible and included a higher content of shrubs (18). Similarly,
328 on the American continent, *B. priscus* adapted to the climatic and environmental changes of the
329 Holocene and evolved in two recently divergent forms, the plain bison thriving on the grasslands of
330 the Great Plains and the wood bison inhabiting the boreal forest in North America. This suggests that
331 on the Eurasian continent the competition with *B. bonasus*, a species seemingly better adapter to a
332 more temperate environment, may have prevented a similar adaptation of *B. priscus* to habitat
333 changes during the warmer periods. Finally, in Western Europe, local variations in ecological and
334 physical barriers could have affected the speed of bison population turnover as a reaction to climatic
335 shifts. In the future, a higher resolution genetic study involving a much higher sample number with

336 denser time and space sampling may provide a more accurate and nuanced view of these population
337 turnovers.

338 The mitochondrial lineages of *B. bonasus* that were present 40 kya have an older root than those
339 of *B. priscus* (250 [287-211] vs 115 [135-95] kya). This indicates that the *B. bonasus* did not experience
340 as severe a bottleneck prior to 100 kya as the population reduction the steppe Bison experienced
341 between 150 and 100 kya, before later thriving in northern Eurasia, Beringia, and in North America
342 between 80 and 20 kya. All the various population expansions and contractions that occurred in
343 response to the climatic and environmental changes characterizing the late Pleistocene and the
344 transition to the Holocene gave rise to a reduction of the population diversity and to the extinction of
345 lineages, like the *Bb1* lineages, which apparently was the first to disappeared, and the *Bp* lineage, which
346 disappeared at the beginning of the Holocene on the Eurasian continent. Finally, the reduction of the
347 diversity of the *Bb2* lineage seems to involve both migrations and local extinctions with the major and
348 most severe reductions occurring between the Early Holocene and historic times, most likely owing to
349 human impact through hunting pressure and habitat fragmentation.

350 Numerous cave art representation in southern France and northern Spain, and also in the Caucasus
351 suggest realistic depictions of both the steppe bison and the wisent (19). We consider likely that the
352 paintings of bison, the so-called “bison of the pillar”, in the cave Chauvet-Pont d’Arc in France depict
353 the two types of bison distinguished by the shape of horns and back lines (Fig. 5). The upper image on
354 the pillar, dated to 38.5-34.1 kya (30), could represent a wisent, and the lower image, dated to 36.2 to
355 34.6 kya (30), a steppe bison. These dates coincide with the period (39 to 34 kya) in which the two
356 bison forms overlap in our dataset from southern France, in the vicinity of these paintings. Within this
357 time frame, wisent population would have been in decline and steppe bison population would have
358 been expanding.

359 Radiation of the *Bos* and *Bison* lineages

360 Since the initial classification of Linnaeus in 1758 of *Bos* and *Bison* within a single genus, there has
361 been debate about whether they should be placed in separate genera (31). Indeed, the members of
362 these genera can still be crossed, despite reduced fertility in some combinations of crosses, and
363 *B. p. taurus* genetic material can be found in a number of present-day American bison and wisent (32,
364 33). Thus, gene flow could have occurred between the various lineages, in particular in the early phases
365 of their differentiation. Such gene flow between separated populations has already been considered
366 as an alternative possibility to incomplete lineage sorting to explain that the mitogenome of *B. p. taurus*
367 was closer to that of *B. bonasus* than to that of *B. bison* (21, 22). The phylogenetic estimates of the age
368 of the various common ancestors of these two lineages indicate, however, that the most parsimonious
369 interpretation of incomplete lineage sorting suffices to account for the relative affiliations of these
370 mitogenomes (see SI Fig. 2). Indeed, as mentioned above, the age estimates indicate that the MRCA of
371 the *Bos* and *Bison* mitogenome lineages is not much older than that of the *B. p. taurus* and *B. bonasus*
372 lineages, respectively 946 [1090-810] kya, and 787 [908-670] kya, with a 35 to 40% overlap of the
373 confidence interval (95% HPD). This indicates that the two bifurcation events have occurred within a
374 relatively short evolutionary period. Rapid speciation during this short evolutionary period appears
375 unlikely since these species have still not yet totally lost interfertility almost a million years later. Our
376 radiation date estimates are within the same range of the earliest fossils that were clearly attributed
377 to the *Bos* genus and that are dated at 1 Mya (34). They are also consistent with the analysis of the
378 complete genome of a modern wisent that estimated that the wisent and bovine species diverged
379 between 1.7 to 0.85 Mya through a speciation process involving an extended period of limited gene
380 flow with some more recent secondary contacts posterior to 150 kya (35). Thus, incomplete lineage
381 sorting of mitogenomes in a metapopulation of the *Bos* and *Bison* ancestors during the period of
382 divergence of these species could account for the affiliation patterns of these mitogenomes without
383 the need to postulate a more recent post-speciation gene flow. It is interesting to note that this
384 radiation event could be coincident with the onset and intensification of high-latitude glacial cycles

385 (100 kyr-periodicity) around 1.2 – 0.8 Mya. Incomplete lineage sorting, however, does not preclude
386 later sporadic introgression of nuclear DNA at any point up to the present owing to the persistent
387 interfertility between these species, as evidenced by the detection in the wisent genome of ancient
388 gene flow from *B. p. taurus* (35, 36).

389 Conclusion

390 The analysis of DNA preserved in ancient bison remains from Eurasia covering the last 50,000 years
391 allowed us to retrace some of the population dynamics that took place during the Late Pleistocene and
392 the Holocene, including population migrations, extinctions and replacements. We could trace back the
393 origin of the wisent to Eastern Europe including the Caucasus. We observed several alternating
394 expansion waves of wisent and steppe bison in Western Europe that were related with climatic
395 fluctuations, the wisent being prevalent when the climate was more temperate leading to a more
396 forested vegetation whereas the steppe bison population originating from northern Eurasia was
397 predominant in Western Europe during the colder periods of the Late Pleistocene with their open
398 environments. These fluctuations may have been recorded in Paleolithic cave paintings, in particular
399 in the cave of Chauvet that had been occupied by humans over a long period and where two distinct
400 bison types are depicted.

401 **Materials & Methods**

402 Details of samples are described in the Supplementary Information (SI Table 1 and SI Fig. 4). All pre-
403 PCR procedures were carried out in the high containment facility of the Jacques Monod Institute
404 physically separated from areas where modern samples are analyzed and dedicated exclusively to
405 ancient DNA analysis using the strict procedures for contamination prevention previously described
406 (37).

407 **DNA Extraction**

408 The external surface of the specimens was removed with a sterile blade to minimize the
409 environmental contamination. For each bone sample, roughly 0.2 g was ground to a fine powder in a
410 freezer mill (Freezer Mill 6750, Spex Certiprep, Metuchen, NJ), which was then suspended in 2mL of
411 extraction buffer containing 0.5M EDTA, 0.25M Di-sodium Hydrogen Phosphate (Na_2HPO_4), pH 8.0,
412 0.14M 2-mercaptoethanol and 0.25 mg/mL of proteinase K and incubated under agitation at 37°C for
413 48 hours. Blank extractions were carried out for each extraction series, eight in total.

414 Samples were then centrifuged and the supernatant was purified with the Qiaquick PCR Purification
415 Kit (Qiagen, Hilden, Germany), as described (37).

416 **PCR Amplification of the HVR**

417 Primers were designed to target conserved regions with minimal primer dimer propensity against
418 a multiple alignment of all the Bison mitochondrial sequences present in Genbank in 2012 using the
419 software Oligo 7 as described (38, 39), and were then tested for efficiency and dimer formation using
420 quantitative real-time PCR (qPCR) (38, 39). Four primer pairs amplifying short (118 to 152 bp)
421 subregions of the mitochondrial Hyper Variable Region (HVR) were selected (SI Table 2 and SI Fig. 1).
422 To protect against cross-contamination between samples, we used the UNG-coupled quantitative real-
423 time PCR system (40) and, to avoid the production of erroneous data due to the presence of bovine
424 DNA in reagents, we decontaminated reagents as previously described (41). Amplifications were
425 performed in a final volume of 10 μL containing 2mM MgCl_2 , 1 μM primers, 0.04mM of dA/G/CTPs and
426 0.08mM of dUTP, 0,01U/ μL of UNG, 1U/ μL of FastStart Taq (Roche Applied Science) and 1 x qPCR

427 home-made reaction buffer (41). Blank amplification controls were included for each amplification. In
428 total, 415 amplification blanks were carried out during the various amplifications analyses of 85
429 samples. No products were observed in any of the amplification blanks. Amplifications were performed
430 using a LightCycler 1.5 (Roche Applied Science) using the following cycling program: 15 minutes at 37°C
431 (carry-over contamination prevention through digestion by UNG of dUTP-containing amplicons), 10
432 minutes at 95°C (inactivation of UNG and activation of the Fast Start DNA polymerase) followed by 60
433 cycles at 95°C for 15 seconds and 60°C for 40 seconds (for primer pairs Bon1, 2 and 3) and 95°C for 15
434 seconds, or 56°C for 15 seconds and 67°C for 20 seconds (for primer pair BB3r4m), followed by a final
435 melting curve analysis step. All extracts were tested for inhibition as previously described (42). Each
436 sequence was determined on both strands from at least two independent amplifications using capillary
437 electrophoresis sequencing. Sequencing data analyses were performed using the software Geneious
438 6.1.8 (43).

439 Capture and sequencing of whole mitogenomes

440 Dual barcoded libraries for Illumina sequencing were constructed using a double-stranded
441 procedure previously described ((37, 44) , see also Supplementary Methods). The End-repair and
442 adapter ligation mixtures were decontaminated with Ethidium monoazide (45) to inactivate bovine
443 DNA associated with BSA present in these reagents that could interfere with the final results. For the
444 production of complete mitogenome sequences, we developed a sequence capture approach using
445 biotinylated RNA baits (46), further detailed in the supplementary information. Briefly, we amplified
446 the *Bos taurus* mitogenome by PCR targeting eleven 1.5 kb-long fragments using primer pairs, one of
447 which contained the T3 promoter as a 5' extension. Strand-specific biotinylated RNA probes were
448 synthesized, pooled and submitted to mild, controlled heat-induced hydrolysis to generate RNA
449 fragments ranging from 100 to 600 nucleotides with an average size of 300. Each library was
450 individually hybridized to the biotinylated probes in the presence of RNA competitors complementary
451 to the Illumina adapters for 48 hours at 62°C. After three 10-min 0.1X SSC washes at 62°C, captured
452 DNA was eluted by alkaline hydrolysis of the RNA probes, amplified an optimal number of PCR cycles

453 as predetermined by qPCR, and subjected to a second round of sequence capture in identical
454 conditions. The eluted DNA was then amplified minimally, purified and sequenced on a MiSeq
455 sequencer (Illumina) using paired-end sequencing for 2x75 cycles.

456 Paired-end reads were merged using leeHom using the --ancientdna parameter (47). Merged reads
457 were then mapped to modern *Bison bison* and *Bison bonasus* mitogenomes using bwa as described in
458 (37). The first 100 nt of each linearized reference mitogenome used for mapping was duplicated at the
459 3'end to allow mapping of fragments overlapping the junction. Mapped read duplicates were then
460 removed using samtools rmdup as described in (37). The resulting bam files were then imported into
461 Geneious 6.1.8 (43) and remapped onto the appropriate mitogenome sequences without the 100 nt
462 duplication (*B. bison* for *B. priscus* sequences, *B. bonasus* for the Bb1 and Bb2 sequences). Consensus
463 sequences were generated in Geneious and verified by visual inspection of the aligned reads.

464 Phylogenetic analyses

465 Sequence alignments were performed using the Muscle algorithm and were visually inspected and
466 adjusted using Geneious 6.1.8 (43) The maximum likelihood (ML) analyses presented in Fig. 1 were
467 computed using PHYML 3.0, using an HKY substitution model with a gamma-distributed rate of
468 variation among sites (+G) and invariant sites (+I) (48). Robustness of the nodes was estimated using
469 500 bootstraps. RaXML 8.2.3 was used to generate the ML bootstrap support values for the complete
470 mitogenome alignment shown in Fig. 3 (49).

471 Phylogenetic analyses conducted under the Bayesian framework were performed using the program
472 BEAST v. 1.8.2, which allows estimation of mutation and population history parameters simultaneously
473 from temporally spaced sequence data (50). Nucleotide substitution models were chosen following
474 comparisons performed with jModelTest 2.1.7 using the Bayesian Information Criteria (51). The HVR
475 analysis presented in Fig. 2 was performed considering a TN93 model for the nucleotide substitution
476 model, a gamma-distributed rate of variation among sites (+G) with four rate categories and invariant
477 sites (i.e., TN93+I+G model). For the complete mitogenome analysis presented in Fig. 3, we used four

478 partitions, the HVR, the 1st and 2nd positions of the codons within the coding region, the 3rd position,
479 and the RNA genes. We considered the HKY+I+G model for the first two partitions, and the TN93+G for
480 the last two. Default priors were used for all parameters of the nucleotide substitution model. For the
481 analysis of figure 2, we used a strict molecular clock with a lognormal prior for the substitution rate
482 (mean=-15.0, stdev=1.4) corresponding to a median of 2E-7 substitutions per site and per year
483 [95%HPD 1.3E-8, 3.2E-6] based on the estimation for Bison HVR substitution rate (7). For the various
484 partitions of the mitogenome of Fig. 3, we used estimates for the human mitogenome substitution
485 rate to set the priors (52): HVR, mean=-16.1 stdev=2.0, corresponding to a median of 1.0E-7 [2E-9-5E-
486 6]; RNA, mean=-18.65 stdev=2.0, corresponding to a median of 8.0E-9 [1.6E-10-4E-7]; 1st & 2nd
487 positions, mean=-18.5 stdev=2.0, corresponding to a median of 9.0E-9 [1.8E-10-4.7E-7]; 3rd position,
488 mean=-17.7 stdev=2.0 corresponding to a median of 2.0E-8 [4E-10-1E-6]. Finally, a standard coalescent
489 model was considered for the tree prior with a Bayesian skyline plot to model populations (5 and 10
490 populations with default parameters for the HVR and the mitogenomes respectively). The prior for the
491 tree height followed a log-normal distribution, mean=14.6 stdev=0.6, truncate to 8.0E6 and 1.0E5,
492 corresponding to a median of 2.2E6 and a 95%HPD of [6.3E6-6.7E5], which integrates the various fossil
493 finds assumed to correspond to ancestors of cattle and bison (53, 54).

494 To estimate the posterior distribution of each parameter of interest, we used the Markov Chain Monte
495 Carlo algorithm implemented in the BEAST software. We ran five independent chains with initial values
496 sampled as described above and an input UPGMA tree constructed using a Juke-Cantor distance
497 matrix. Each of these chains was run for 50,000,000 iterations and for each parameter of interest,
498 18,000 samples (one every 2,500 generated ones) were drawn after discarding a 10% burn-in period.
499 The BEAST output was analyzed with the software Tracer v. 1.6
500 <http://tree.bio.ed.ac.uk/software/tracer/>. Visual inspection of the traces and the estimated posterior
501 distributions suggested that each MCMC had converged on its stationary distribution. Using
502 Logcombiner v. 1.8.2, we further combined all the results from the 5 independent chains. The

503 maximum clade credibility tree with the median height of the nodes was finally calculated using
504 TreeAnnotator v. 1.8.2 and visualized using FigTree v. 1.4.2 <http://tree.bio.ed.ac.uk/software/figtree/>.

505 **Acknowledgments**

506 The study was supported by the French national research center CNRS. The paleogenomic facility
507 obtained support from the University Paris Diderot within the program “Actions de recherche
508 structurantes”. The sequencing facility of the Institut Jacques Monod, Paris, is supported by grants
509 from the University Paris Diderot, the Fondation pour la Recherche Médicale (DGE20111123014), and
510 the Région Ile-de-France (11015901). We thank Lou Saïer for the production of HVR data for some
511 samples. We acknowledge the contribution to sampling of Myriam Boudadi-Maligne, Jean-Baptiste
512 Mallye, Pierre Pétrequin, Sylvie Lourdaux, and René Rémond. We thank G. Baldacci for continuous
513 support. M. T. also acknowledges financial support through the “Biodiversity of East-European and
514 Siberian large mammals on the level of genetic variation of populations (BIOGEAST)” project within the
515 7th Framework Programme, Marie Curie Actions, that allowed sampling to take place in Russia. We
516 like to thank Marie-Hélène Moncel and Marie-Anne Julien for providing samples that did not yield
517 genetic results, and the French ministry of culture for providing the image of the wall paintings of the
518 Chauvet cave.

519 **Author Contributions**

520 EMG and TG designed and supervised the overall research with an initial input from MT. DM
521 developed sequence capture and produced the mitogenome data. SG produced the HVR data. TG,
522 EMG, DM and SG analyzed and interpreted the data. TG, EMG and EAB wrote the manuscript with
523 inputs from DM and SG. JPB provided samples, discussed the data and corrected the manuscript. MT,
524 RMA, GBa, GBo, JCC, SM, OP, NS and HPU provided samples and feedbacks on the manuscript.

525 Bibliography

526

- 527 1. Hewitt GM (2004) Genetic consequences of climatic oscillations in the Quaternary. *Phil.*
528 *Trans. RL. Soc. Lond. B* 359:183-195.
- 529 2. Markova AK, *et al.* (2015) Changes in the Eurasian distribution of the musk ox (*Ovibos*
530 *moschatus*) and the extinct bison (*Bison priscus*) during the last 50 ka BP. *Quatern Int* 378:99-
531 110.
- 532 3. Guthrie RD (1990) *Frozen fauna of the Mammoth Steppe. The story of Blue Babe.* (The
533 University of Chicago Press, Chicago and London) p 323.
- 534 4. Brugal JP (1994-1995) Le Bison (Bovinae, Artiodactyla) du gisement Pléistocène moyen
535 ancien de Durfort (Gard, France). *Bull.Mus.nat.Hist.Nat., Paris* 4é sér. 16, sect.C, n°2-4:349-
536 381.
- 537 5. Brugal JP, David F, Enloe J, & Jaubert J (1999) *Le Bison, gibier et moyen de subsistance des*
538 *hommes du Paléolithique aux Paléindiens des grandes plaines* (Antibes).
- 539 6. Flerow CC (1979) Systematics and Evolution. *European Bison -Morphology, systematics,*
540 *evolution, ecology (in Russian)*, , ed Sokolov VE (Nauka (USSR Ac. of Sc.), Moscou), pp 9-127
- 541 7. Shapiro B, *et al.* (2004) Rise and fall of the Beringian steppe bison. *Science* 306(5701):1561-
542 1565.
- 543 8. Groves CP (1981) Systematic relationship in the Bovini (Artiodactyla, Bovidae).
544 *Z.Zool.Syst.Evolutionforsch.* 19(4):264-278.
- 545 9. Hassanin A, An J, Ropiquet A, Nguyen TT, & Couloux A (2013) Combining multiple autosomal
546 introns for studying shallow phylogeny and taxonomy of Laurasiatherian mammals:
547 Application to the tribe Bovini (Cetartiodactyla, Bovidae). *Molecular phylogenetics and*
548 *evolution* 66(3):766-775.
- 549 10. Kowalski K (1967) The evolution and fossil remains of the European Bison. *Acta Theriologica*
550 12(21):335-338.
- 551 11. Krasnińska M & Krasniński ZA (2013) *European Bison: The Nature Monograph. 2nd Edition*
552 (Springer, Heidelberg).
- 553 12. Cooper A, *et al.* (2015) PALEOECOLOGY. Abrupt warming events drove Late Pleistocene
554 Holarctic megafaunal turnover. *Science* 349(6248):602-606.
- 555 13. Boeskorov GG, *et al.* (2014) Preliminary analyses of the frozen mummies of mammoth
556 (*Mammuthus primigenius*), bison (*Bison priscus*) and horse (*Equus* sp.) from the Yana-
557 Indigirka Lowland, Yakutia, Russia. *Integrative zoology* 9(4):471-480.
- 558 14. Kirillova IV, *et al.* (2015) An ancient bison from the mouth of the Rauchua River (Chukotka,
559 Russia). *Quatern. Res.* 84(2):232-245.
- 560 15. Degerbøl M & Iversen J (1945) *The Bison in Denmark. A zoological and geological*
561 *investigation of the finds in Danish Pleistocene deposits* (Danm.Geol.Undersøgelse,
562 Copenhagen).
- 563 16. Geist V (1971) The relation of social evolution and dispersal in ungulates during the
564 Pleistocene, with emphasis on the old world Deer and the genus *Bison*. *Quaternary Research*
565 1(3):283-221.
- 566 17. Rautian GS, Kalabushkin BA, & Nemtsev AS (2000) A New Subspecies of the European Bison,
567 *Bison bonasus montanus* ssp. nov. (Bovidae, Artiodactyla). *Doklady Biological Sciences* 375
568 636–640.
- 569 18. Bocherens H, Hofman-Kaminska E, Drucker DG, Schmolcke U, & Kowalczyk R (2015) European
570 bison as a refugee species? Evidence from isotopic data on Early Holocene bison and other
571 large herbivores in northern Europe. *PLoS One* 10(2):e0115090.
- 572 19. Spassov N & Stovtechev T (2003) On the origin of the wisent, *Bison bonasus* (Linnaeus, 1758)
573 : presence of the wisent in the upper Palaeolithic art of Eurasia. *Advances in Vertebrate*
574 *Paleontology « Hen to Panta »*:125-130.

- 575 20. Potter BA, *et al.* (2010) History of Bison in North America. *American Bison: Status survey and*
576 *conservation guidelines 2010*, eds Gates CC, Freese CH, Gogan PJP, & Kotzman M (IUCN,
577 Gland, Switzerland), pp 13-18.
- 578 21. Verkaar EL, Nijman IJ, Beeke M, Hanekamp E, & Lenstra JA (2004) Maternal and paternal
579 lineages in cross-breeding bovine species. Has wisent a hybrid origin? *Mol Biol Evol*
580 21(7):1165-1170.
- 581 22. Zeyland J, *et al.* (2012) Tracking of wisent-bison-yak mitochondrial evolution. *Journal of*
582 *applied genetics* 53(3):317-322.
- 583 23. Marsolier-Kergoat MC, *et al.* (2015) Hunting the Extinct Steppe Bison (*Bison priscus*)
584 Mitochondrial Genome in the Trois-Freres Paleolithic Painted Cave. *PLoS One*
585 10(6):e0128267.
- 586 24. Lisiecki LE & Raymo ME (2005) A Pliocene-Pleistocene stack of 57 globally distributed benthic
587 $\delta^{18}O$ records. *Paleoceanography* 20(1):1-17.
- 588 25. Andersen KK, *et al.* (2004) High-resolution record of Northern Hemisphere climate extending
589 into the last interglacial period. *Nature* 431(7005):147-151.
- 590 26. Van Andel TH & Tzedakis PC (1996) Palaeolithic landscapes of Europe and environs, 150,000-
591 25,000 years ago: An overview. *Quat Sci Rev* 15(5-6):481-500.
- 592 27. Guiot J, Pons A, de Beaulieu JL, & Reille M (1989) A 140,000 year climatic reconstruction from
593 two European pollen records. *Nature* 338: 309-313.
- 594 28. Palombo MR (2014) Deconstructing mammal dispersals and faunal dynamics in SW Europe
595 during the Quaternary. *Quat Sci Rev* 96:50-71.
- 596 29. Julien M-F, *et al.* (2012) Were European steppe bison migratory? ^{18}O , ^{13}C and Sr intra-tooth
597 isotopic variations applied to a palaeoethological reconstruction. *Quaternary International*
598 271:106-119.
- 599 30. Quiles A, *et al.* (2016) A high-precision chronological model for the decorated Upper
600 Paleolithic cave of Chauvet-Pont d'Arc, Ardeche, France. *Proc Natl Acad Sci U S A*
601 113(17):4670-4675.
- 602 31. Boyd DP, Wilson GA, & Gates CC (2010) Taxonomy and nomenclature. *American Bison: Status*
603 *survey and conservation guidelines 2010*, eds Gates CC, Freese CH, Gogan PJP, & Kotzman M
604 (IUCN, Gland, Switzerland), pp 13-18.
- 605 32. Yudin NS, *et al.* (2012) Detection of mitochondrial DNA from domestic cattle in European
606 bison (*Bison bonasus*) from the Altai Republic in Russia. *Anim Genet* 43(3):362.
- 607 33. Halbert ND & Derr JN (2007) A comprehensive evaluation of cattle introgression into US
608 federal bison herds. *The Journal of heredity* 98(1):1-12.
- 609 34. Martínez-Navarro B, Rook L, Papini M, & Libsekal Y (2010) A new species of bull from the
610 Early Pleistocene paleoanthropological site of Buia (Eritrea): Parallelism on the dispersal of
611 the genus *Bos* and the Acheulian culture. *Quatern Int* 212(2):169-175.
- 612 35. Gautier M, *et al.* (2016) Deciphering the wisent demographic and adaptive histories from
613 individual whole-genome sequences. *Mol Biol Evol* In press, biorxiv
614 <http://dx.doi.org/10.1101/058446>.
- 615 36. Wecek K, *et al.* (2016) Complex admixture preceded and followed the extinction of wisent in
616 the wild. *bioRxiv* 059527:doi: <http://dx.doi.org/10.1101/059527>
- 617 37. Bennett EA, *et al.* (2014) Library construction for ancient genomics: single strand or double
618 strand? *BioTechniques* 56(6):289-290, 292-286, 298, passim.
- 619 38. Cote NM, *et al.* (2016) A New High-Throughput Approach to Genotype Ancient Human
620 Gastrointestinal Parasites. *PLoS One* 11(1):e0146230.
- 621 39. Guimaraes S, *et al.* (submitted) A cost-effective high-throughput metabarcoding approach
622 powerful enough to genotype ~44,000 year-old rodent remains from Northern Africa.
623 *Molecular Ecology Resources*.
- 624 40. Pruvost M, Grange T, & Geigl E-M (2005) Minimizing DNA contamination by using UNG-
625 coupled quantitative real-time PCR on degraded DNA samples: application to ancient DNA
626 studies. *BioTechniques* 38(4):569-575.

- 627 41. Champlot S, *et al.* (2010) An efficient multistrategy DNA decontamination procedure of PCR
628 reagents for hypersensitive PCR applications. *PLoS ONE* 5(9).
- 629 42. Pruvost M, *et al.* (2007) Freshly excavated fossil bones are best for amplification of ancient
630 DNA. *Proc. Natl. Acad. Sci. USA* 104(3):739-744.
- 631 43. Kearse M, *et al.* (2012) Geneious Basic: an integrated and extendable desktop software
632 platform for the organization and analysis of sequence data. *Bioinformatics* 28(12):1647-
633 1649.
- 634 44. Gorge O, *et al.* (2016) Analysis of Ancient DNA in Microbial Ecology. *Methods in molecular
635 biology* 1399:289-315.
- 636 45. Rueckert A & Morgan HW (2007) Removal of contaminating DNA from polymerase chain
637 reaction using ethidium monoazide. *Journal of microbiological methods* 68(3):596-600.
- 638 46. Gnirke A, *et al.* (2009) Solution hybrid selection with ultra-long oligonucleotides for massively
639 parallel targeted sequencing. *Nature biotechnology* 27(2):182-189.
- 640 47. Renaud G, Stenzel U, & Kelso J (2014) leeHom: adaptor trimming and merging for Illumina
641 sequencing reads. *Nucleic Acids Res* 42(18):e141.
- 642 48. Guindon S, *et al.* (2010) New algorithms and methods to estimate maximum-likelihood
643 phylogenies: assessing the performance of PhyML 3.0. *Systematic biology* 59(3):307-321.
- 644 49. Stamatakis A (2014) RAxML version 8: a tool for phylogenetic analysis and post-analysis of
645 large phylogenies. *Bioinformatics* 30(9):1312-1313.
- 646 50. Drummond AJ & Rambaut A (2007) BEAST: Bayesian evolutionary analysis by sampling trees.
647 *BMC Evolutionary Biology* 7:214.
- 648 51. Darriba D, Taboada GL, Doallo R, & Posada D (2012) jModelTest 2: more models, new
649 heuristics and parallel computing. *Nature methods* 9(8):772.
- 650 52. Soares P, *et al.* (2009) Correcting for purifying selection: an improved human mitochondrial
651 molecular clock. *Am J Hum Genet* 84(6):740-759.
- 652 53. Martínez-Navarro B, Ros-Montoya S, Espigares MP, & Palmqvist P (2011) Presence of the
653 Asian origin Bovini, *Hemibos* sp. aff. *Hemibos gracilis* and *Bison* sp., at the early Pleistocene
654 site of Venta Micena (Orce, Spain). *Quatern Int* 243(1):54-60.
- 655 54. Qui Z, Deng T, & Wang B (2004) Early Pleistocene mammalian fauna from Longdan, Dongxian,
656 Gansu, China. *Paleontologia Sinica* 191(C27):1-198.

657

658 Legends to Figures

659 Fig. 1 Maximum Likelihood phylogeny of the ancient Bison hypervariable region

660 ML analyses of the HVR produced in this study using PHYML, a HKY+I+G substitution model and 500
661 bootstraps. The bootstrap support of the nodes is indicated in red. The geolocalization of the analyzed
662 samples is represented using a color code to distinguish five origins and time periods as represented
663 on the Eurasiatic continent map (see SI. Fig.4 for a map of the distribution of the Western European
664 sites). Three clades can be clearly distinguished, the *Bison priscus* (*Bp*) clade and two *Bison bonasus*
665 clades (*Bb1* and *Bb2*). The scale corresponds to the number of nucleotide substitutions per site. The
666 samples that have allowed amplification of all 4 PCR fragments as represented in SI fig. 1 are indicated
667 by the suffix *_C* whereas those for which one or more fragments were missing are indicated by the
668 suffix *_NC*. The stars indicate the samples that were used for the full mitogenome analysis presented
669 in Fig. 3.

670 Fig. 2: Bayesian phylogeny of Bison hypervariable region

671 All dated and complete ancient Bison sequences produced here and in a previous *B. priscus* analysis
672 (7) were aligned and reduced to the 367 bp sequence targeted herein alongside modern *B. bonasus*
673 and *B. bison* sequences. A Bayesian phylogenetic analysis was performed using Beast to estimate the
674 age of the nodes from temporally spaced sequence data. The age of the nodes (in kya) is indicated in
675 red, whereas the blue bars represent the 95% HPD of these ages. The color code representing the
676 origin of the various samples is as indicated. The inset on the lower part of the figure represents a
677 magnified view of the *B. bonasus* branches of the tree. The posterior probability of the nodes is
678 indicated in blue and the thickness of the branches is proportional to this posterior probability.

679 Fig. 3: Bayesian phylogeny of complete mitogenomes of *Bos* and *Bison*.

680 We used the complete mitogenomes of ancient *Bison* obtained herein as well as the two published
681 *B. priscus* mitogenomes, and all modern *Bison bison*, *Bison bonasus*, *Poephagus grunniens*, and *Bos*
682 *primigenius taurus* mitogenomes available in Genbank in 2015 totaling 439 sequences. The *B. bison*,
683 *P. grunniens* and *B. p. taurus* sequences have been collapsed to preserve only their subclade structure.

684 The estimate of the age of the nodes, in kya, are indicated in red, with the 95% HPD indicated by blue
685 bars. The statistical supports of the nodes are indicated in blue (Bayesian posterior probability) and in
686 green (bootstrap values of a ML phylogeny performed using RaXML).

687 **Fig. 4: Schematic representation of the distribution through time and space of the**
688 **various mitogenome clades**

689 The geographic regions are represented on the abscissa and the time scale on the ordinate. The
690 ascertained presence of the various mitochondrial haplogroups are represented by solid boxes,
691 whereas the dotted lines indicate possible temporal extension of the presence of these clades. The left
692 side shows the climatic fluctuations as inferred from the North Greenland Ice Core Project (NGRIP) (25)
693 and the combined Carabean Cariaco basin and NGRIP data as shown in (12), as well as the Marine
694 Isotope Stage (MIS) as defined by Lisiecki and Raymo²⁴ (http://www.lorraine-lisiecki.com/LR04_MISboundaries.txt). The proposed migrations are indicated by solid arrows. The
695 hatched arrow indicates a possible migration of the *Bb1* clade that populated Western Europe from a
696 southern refugee before the time period analyzed herein. The genetic identity of the bison that,
697 according to the fossil record, populated Western Europe before 60 kya is not known, but climatic
698 fluctuations may have triggered additional expansions and contractions of different populations of
699 *B. priscus* and *B. bonasus*. (Drawings: E.-M. Geigl)

701 **Fig. 5: Prehistoric painting of bison in the cave of Chauvet-Pont d'Arc, Ardèche,**
702 **France**

703 The paintings are the so-called "Bison of the pillar" in the "End Chamber" of the Chauvet cave. The
704 charcoal of both drawings have been radiocarbon dated at 38.5-34.1 kya for the upper bison, and at
705 36.3-34.6 kya for the lower bison (30). We consider, based on criteria stated by Spassov (19) that the
706 "great bison" in the upper part represents *B. bonasus* with a highly positioned head, curved horns, a
707 moderately large hump and a weak mane and rather equilibrated body proportions between the
708 front and the rear. The lower part would represent *B. priscus* with its large hump, its low head
709 position, its abundant mane, crescent-shaped horns, and, although somewhat faded in the image,

- 710 the steep incline of the back-line and stronger hindquarters can be made out. (Copyright: French
711 Ministry of culture, archeologie.culture.fr/chauvet. Cl. Arnaud Frich. CNP/MCC)

Population	Nind	Nhap	Haplotype diversity, <i>H</i>	Nucleotide diversity, <i>Pi</i>	Theta(k)	Theta(S)	Theta(Pi)	Theta (per site)
Upper Pleistocene Siberia (Bp)	4	4	1.00 ± 0.18	0.046 ± 0.031	*	15.82± 8.85	16.83 ± 9.55	0.044
Upper Pleistocene Europe (Bp)	4	4	1.00 ± 0.18	0.014 ± 0.010	*	4.91 ± 2.97	5.17 ± 3.77	0.014
Upper Pleistocene Caucasus (Bb1-Bb2)	7	7	1.00 ± 0.08	0.078 ± 0.045	*	23.67 ± 10.92	28.95 ± 16.57	0,068
Holocene Europe (ancient, Bb2)	5	3	0.80 ± 0.16	0.010 ± 0.007	2.22	4.32 ± 2.48	3.80 ± 2.68	0,012
Modern Europe (Pre-WWI, Bb2)	19	3	0.51 ± 0.12	0.001 ± 0.001	0.73	0.57 ± 0.43	0.56 ± 0.53	0,0016
Modern Caucasus (Pre-WWI, Bb2)	4	2	0.67 ± 0.20	0.002 ± 0.002	0.88	0.54 ± 0.54	0.67 ± 0.75	0,0015

Pairwise Nucleotide divergence with Jukes and Cantor calculated with DNAsp

	Upper Pleistocene Siberia	Upper Pleistocene Europe	Upper Pleistocene Caucasus	Holocene Europe (ancient)	Modern Europe	Modern Caucasus
Upper Pleistocene Siberia	*					
Upper Pleistocene Europe	0.03712	*				
Upper Pleistocene Caucasus	0.21127	0.19816	*			
Holocene Europe (ancient)	0.19524	0.18988	0.07614	*		
Modern Europe	0.18548	0.17621	0.07498	0.01797	*	
Modern Caucasus	0.18306	0.17443	0.07506	0.02128	0.00367	*

Calculations relied only on the samples that yielded the four PCR fragments

Table 1

Age estimates of the nodes (kya)		
Node	Age from HVR [95% HPD]	Age from mitogenome [95% HPD]
Root Bovina	1080 [1550-700]	944 [1090-810]
Bos Taurus/B. bonasus	-	786 [908-668]
B. indicus/B. taurus	-	161 [189-133]
B. grunniens/B. priscus	-	328 [378-272]
B. priscus	151 [193-119]	115 [135-95]
B. bison	21 [27-16]	12 [14-7]
All B. bonasus	438 [643-284]	250 [287-211]
B. bonasus Bb2	105 [158-75]	87 [97-75]

Clock rate estimates (per site * year)		
Partition	Rate from HVR [95% HPD]	Rate from mitogenome [95% HPD]
HVR	5.4 [3.9-6.9] E-7	4.6 [3.7-5.6] E-7
RNA	-	2.5 [2.1-2.9] E-8
Coding (1st-2d positions)	-	2.6 [2.2-3.0] E-8
Coding (3d position)	-	9.1 [7.8-10.5] E-8

Table 2

Figure 1

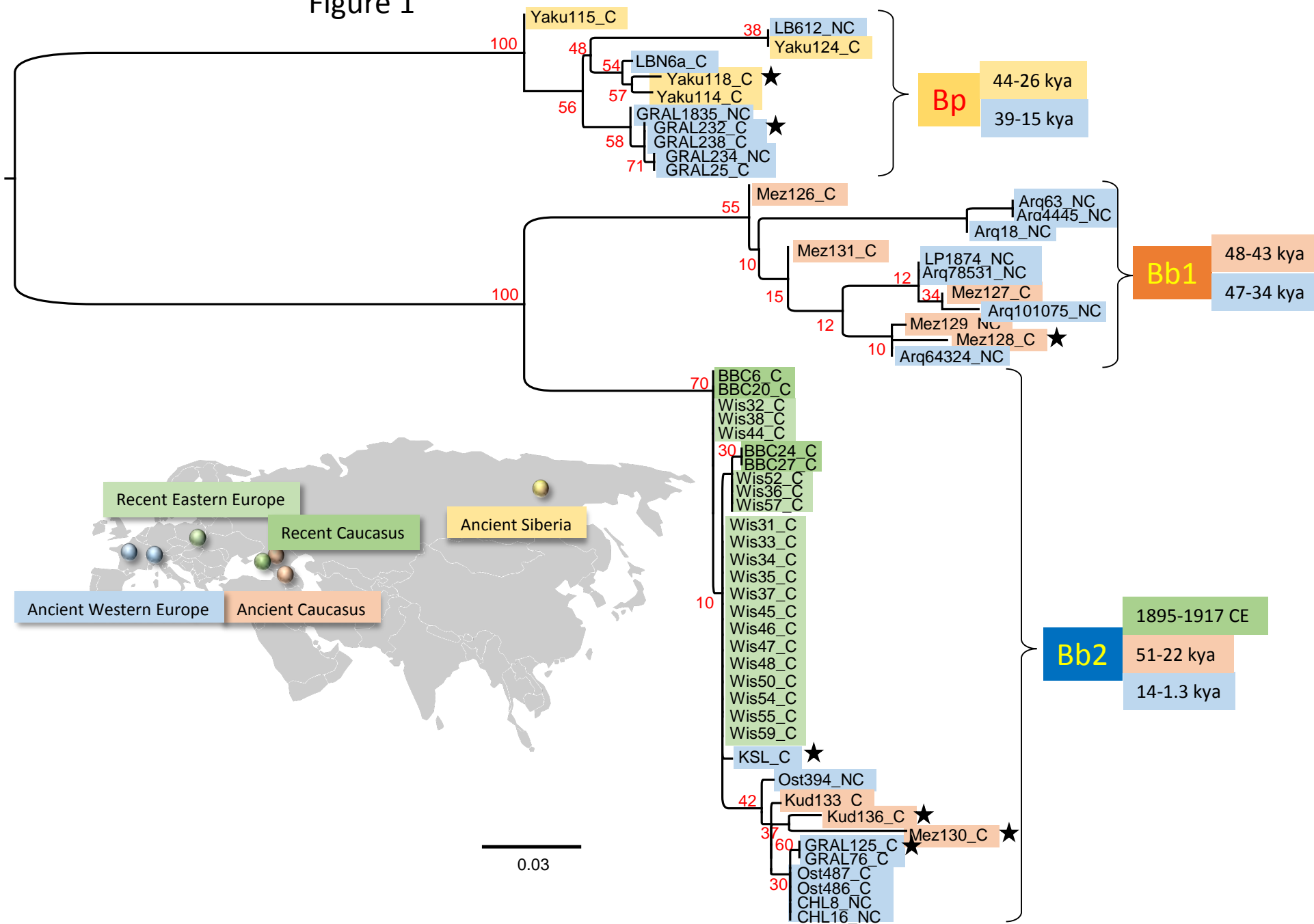


Figure 3

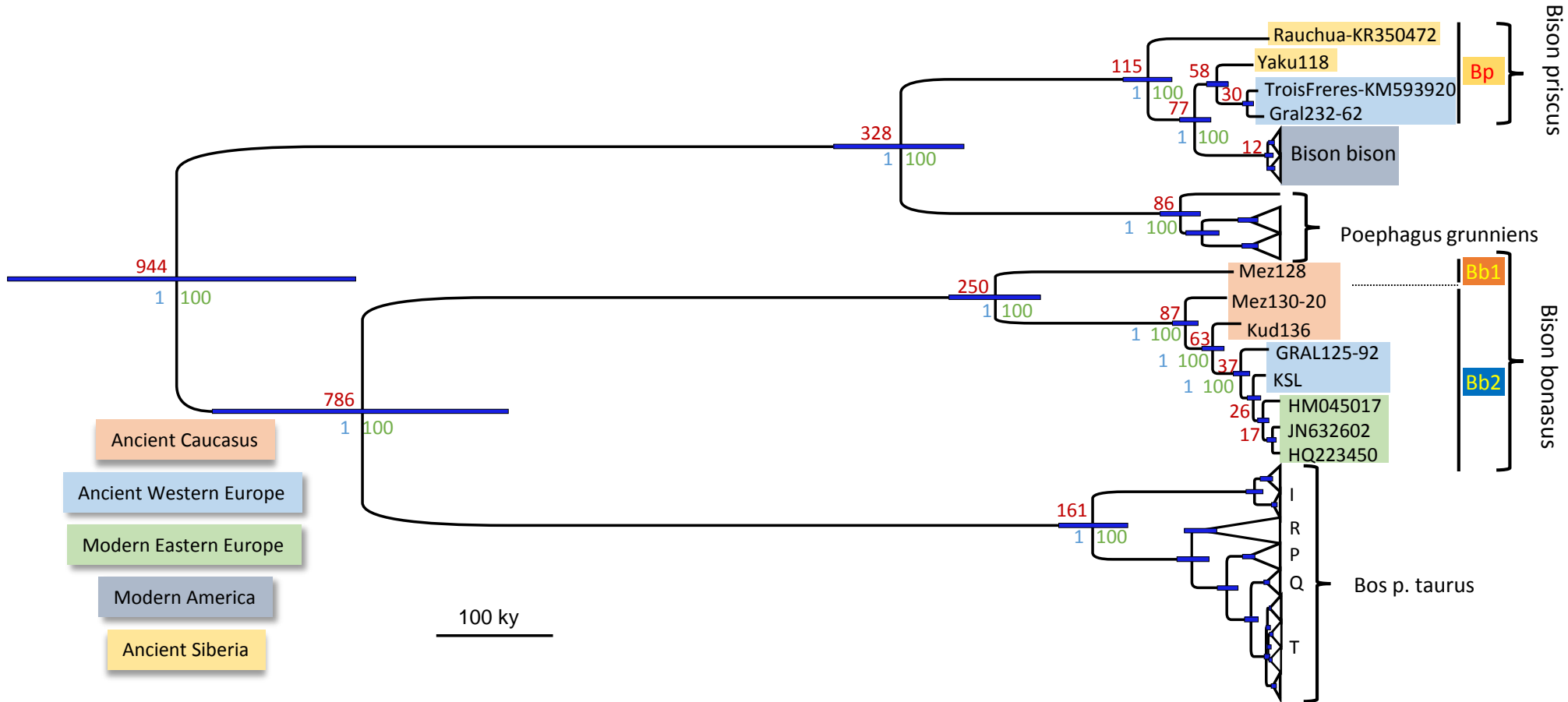


Figure 4

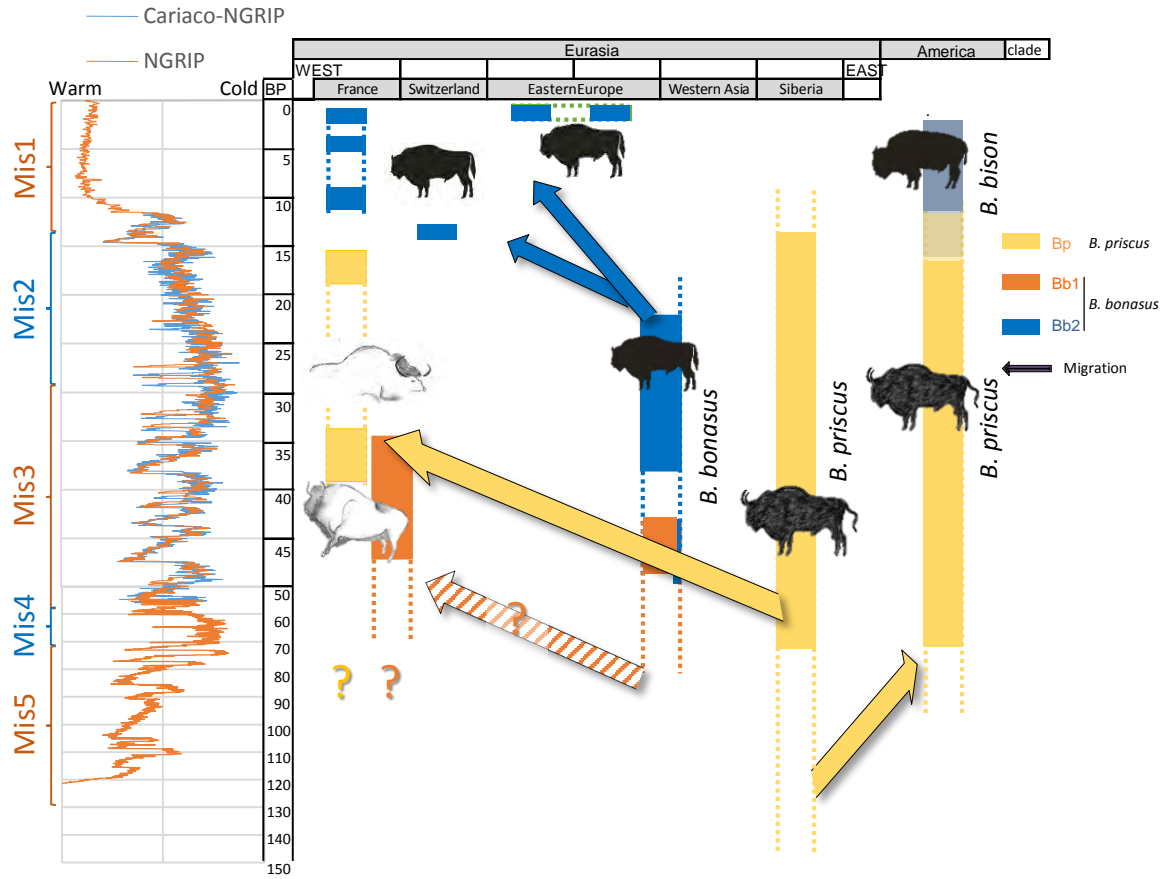


Figure 5

